Available online at www.sciencedirect.com

ScienceDirect

MATTER AND RADIATION AT EXTREMES

Matter and Radiation at Extremes 2 (2017) 177−189

www.journals.elsevier.com/matter-and-radiation-at-extremes

Research Article

Non-thermal laser driven plasma-blocks for proton boron avalanche fusion as direct drive option

Heinrich Hora [a,*], Shalom Eliezer [b], Noaz Nissim [b], Paraskevas Lalousis [c]

[a] *Department of Theoretical Physics, University of New South Wales, Sydney, Australia*
[b] *Soreq Research Center, Yavne, Israel*
[c] *Institute of Electronic Structure and Laser FORTH, Heraklion, Greece*

Received 10 December 2016; revised 25 April 2017; accepted 5 May 2017
Available online 26 May 2017

Abstract

Fusion energy from protons reacting with ^{11}B, HB11, is extremely difficult or impossible when using thermal ignition by laser irradiation. This changes radically when using picosecond laser pulses with powers above petawatts dominated by nonlinear force driven ultrahigh acceleration of plasma blocks for a non-thermal initiation of igniting solid density HB11 fuel. For a cylindrical trapping of the reaction, laser produced ultrahigh magnetic fields above kiloTesla, have to be combined. The experimentally confirmed highly increased HB11 fusion gains due to avalanche reaction may lead to a scheme of an environmentally clean and economic power reactor.

PACS Codes: 52.38.-r; 52.57.-z; 52.57.Fg

Keywords: Boron laser fusion; Plasma-block ignition; ultrahigh acceleration; Kilotesla field trapping; Avalanche reaction; Power reactor

1. Introduction

The main source of energy on earth is the irradiation from the sun based on the fusion reaction of hydrogen into helium, where a change of mass Δm results in a conversion of energy according to Einstein's Δmc^2 relation with the vacuum light velocity c. This energy generation was first produced on earth on 1 November 1952 [1] by a reaction of heavy hydrogen D with superheavy hydrogen tritium T (DT-fusion) in an explosive way. For a controlled fusion in a power reactor, extensive efforts are on the way since about 1950 where the reacting high temperature DT plasma has to be trapped by magnetic fields, as magnetic confinement fusion MCF resulting in the ITER [2] or Stellarator [3] project where the highest achieved gains [4] are still below break-even.

With the advent of the laser in 1960, the possibility to extremely concentrate light energy within extremely short times opened another option in contrast to MCF by studying inertial confinement fusion ICF [5−7]. The DT fusion is known as the easiest reaction but has the disadvantage that compared to the production of harmless helium, neutrons are generated causing pollution by radioactive radiation. An alternative reaction without neutron generation is the fusion of light hydrogen with boron isotope 11 (HB11 reaction). Every expert knows that this fusion is extremely difficult and practically impossible for a fusion reactor. Since 2009 it is known [8,9] that a non-thermal reaction driven by laser pulses of extremely high power reduces the difficulty of HB11 by many orders of magnitude to the same level as DT. This method [10,11] becomes known as plasma block ignition [12,13] facilitating the ignition by direct drive using the dominance of ponderomotive forces [8,13,14] in need of a combination

* Corresponding author.
E-mail address: h.hora@unsw.edu.au (H. Hora).
Peer review under responsibility of Science and Technology Information Center, China Academy of Engineering Physics.

http://dx.doi.org/10.1016/j.mre.2017.05.001

with the recent developments of ultrahigh magnetic fields [15]. The long expected avalanche HB11 reaction [16] with measured highly elevated gains [17,18] could be recognized to result in the avalanche mechanism [19,20] and could be followed up in details by an elastic ion collision mechanism [21].

The way to discuss the new scheme of a fusion reactor for clean, low cost and lasting electric power generation needs an explanation of the special conditions of a direct drive mechanism with the ultrahigh power laser pulses for the ignition. This is the reason why the steps of how direct drive is developed compared with other driving schemes needs a broader attention. This appears now in some contrast to the picosecond initiation process for the laser ignition of the fusion, see Sec. 4 and after for more details.

2. Indirect drive ICF and spark ignition

The scheme of indirect drive ICF goes back to the studies by John Nuckolls in early 1960 [22] when he had results from supercomputer calculations about radiation driven DT micro-fusion explosions. The radiation was projected to be driven within an explosion chamber to be incident on DT masses as less as 1 mg. This was just few months before the laser was discovered [23] whose radiation was considered as the best source for the radiation ignition of a micro explosion. This could be experimentally verified [24] by underground experiments if the X-ray of more than 10 MJ energy was used from nuclear explosions to irradiate a fusion target resulting in a considerable high gain of energy production above the incident radiation. This was the demonstration of an energy source for a controlled nuclear power generation in a reactor. It demonstrated that the fusion power station was at hand, if the igniting radiation was generated by a laser.

The way of how to develop the necessary laser pulses is well summarized [25,26] while the optimization of the conditions [27] of the irradiated fuel for the best possible reaction gain [28−30] strongly depends on the reheat by the generated alpha particles within the reacting plasma (see more in Sec. 3). Gains of DT fusion are given by the generated neutrons as Fig. 1 [31] depending on the energy of laser pulses irradiated with the duration in the nanosecond range. The highest gains are given by indirect drive when the laser radiation is incident into capsules onto their inner walls for change into X-ray radiation for interacting of fusion fuel sphere in the center to produce nuclear reactions as initially described by Nuckolls [32] and measured in underground experiments [24] with high gains.

The further main aim of indirect drive is to use a fuel target with special spherical design of layers for a spark ignition in order to increase the gain when irradiating a sophisticated time dependence of the laser pulse with the capsule and the fusion fuel target in the center. The reaction should then be a spark ignition [33] as explained in an early computation [34].

The irradiating laser produces a central spark of high temperature and modest density within a high density low temperature mantle of DT fusion fuel (see Fig. 2). At the boundary of the hot spot to the mantle, the spark reaction produces a fusion detonation front into the mantle for reaching a maximum energy gain of the reaction. An evaluation is using the following approximations. Instead of the curved radial temperature and density profiles (see Fig. 2), at the stage of the highest compression in the center, we select an averaged inner spark region of 250 times of the solid-state density n_s, and temperature 10 keV (maximum 12 keV), changing at the detonation-front radius $0.47r_0$ into an outer region with average temperature 400 eV and density $1000n_s$ (maximum $2300n_s$). The plasma radius at the highest compression is derived from gains based on an initial radius $r_0 = 3$ mm at a time before compression. The efficiency f of the fusion detonation wave going through the outer high-density, low-temperature DT plasma after being triggered by the inner spark is rather low according to the Fraley−Linnebur−Mason−Morse formula [35,36] using

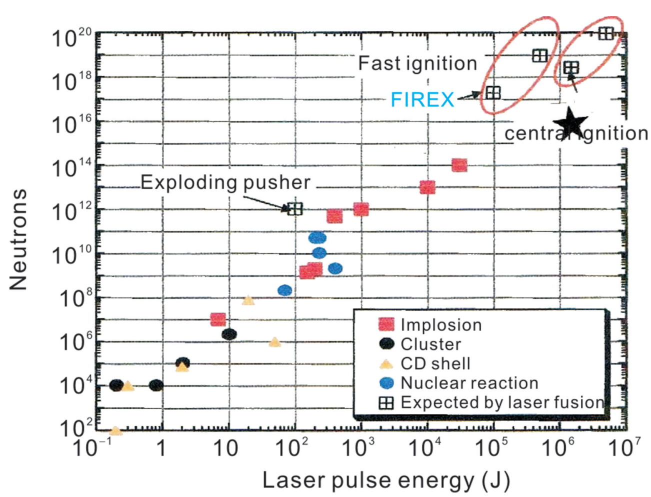

Fig. 1. Measured highest neutron gains N per incident laser energy (full signs) with the highest value reported [28] given by an asterisk [31].

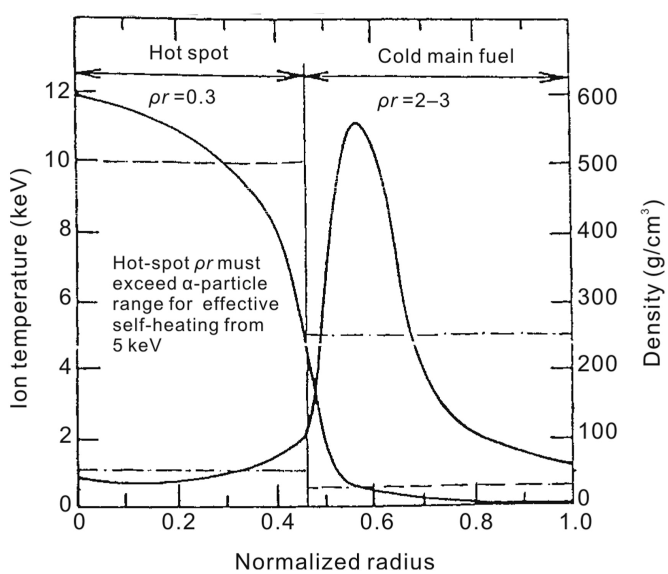

Fig. 2. Radial profiles of the ion temperature and density in a DT pellet computed at highest compression for isobaric spark ignition [34] for incident 10 MJ laser energy producing 1 GJ fusion energy using spark ignition. The radius of the fusion detonation wave is 0.47 of the actual plasma radius; the dashed lines are the average temperatures of the inner and outer regions and the dashed-dotted lines are the averages of the respective densities.

$H = \rho R = 2$ (see Fig. 2), and $H_B = 7\ \text{g}\cdot\text{cm}^{-2}$. The total fuel depletion (fuel consumption) is then only 18.9%, giving a total gain $G_L = 100$ for 10 MJ laser energy, assuming $\eta = 10\%$, the hydrodynamic efficiency, which is defined as the ratio of energy E_0 that goes into the compressed DT plasma core of a radius less than r_0 divided by energy E_L of the incident laser pulse. All of these values are reasonably close to the detailed computation of Storm et al. [34], where, instead of our averaged values, the computed density and temperature profiles are shown for the used conditions of an isobaric compression.

$$f = \frac{H}{H + H_B} = 22\%, \tag{1}$$

For reaching improved conditions for a fusion reactor, the advantage of fine modifications of the laser pulses is aimed in contrast to the brute force X-ray pulses from the underground experiments [24]. The analysis of direct drive laser fusion (see Sec. 3) explains how sensible the selection of the parameters is for modifying the laser pulses. This is in similar way also valid for indirect drive as can be understood from measured properties. Taking these modifications into account, there is a considerable potential available for reaching the sufficiently high gain conditions of the laser fusion reactor. The study of the indirect drive for reactor conditions is based on the fact, that the inertial fusion reactor has been shown to work in principle with the X-ray (regrettably still very high >10 MJ energy pulses for ignition) underground experiments with further improvements by a sophisticated modification of the nanosecond type laser pulse irradiation and by appropriately adjusted spark ignition targets for more relaxed conditions. These fully demonstrated facts are the basis to follow up this ignition.

3. Direct drive and volume ignition

Direct drive uses the interaction of a laser pulse on initially uniform fusion fuel. At spherical geometry − different to plane geometry in the cases with picosecond laser irradiation in the last section − the compact fuel can be compressed adiabatically according to the hydrodynamic self-similarity properties where the generation of shocks has to be avoided. The compression of the fuel up to a maximum density n in multiples of the solid state density n_0 is then calculated for a laser energy E_0 deposited into the sphere of a radius R_0 before compression as recoil reaction from the ablation of the surface layer. A general value for the efficiency is that about 5% of the irradiated laser energy goes into the compressed core as "core energy" E_0 while 95% is needed for the ablation-compression mechanism. In Fig. 2, the lower left hand part shows dashed parabolas of the resulting fusion energy gain G per core energy from the laser pulse for DT fuel in a volume V_{0s} of the solid state density before compression. For a parabola, the core energy E_0 is too low, the reached temporally changing temperature at adiabatic compression is too low for high gains. On the other hand, if the core energy is very high, the fusion gain G is lower because the adiabatic expansion of the fuel is too fast to produce a good gain.

Taking parabolas for varying V_{0s} where the maximum compression n/n_s is the same, results in a set with a tangent

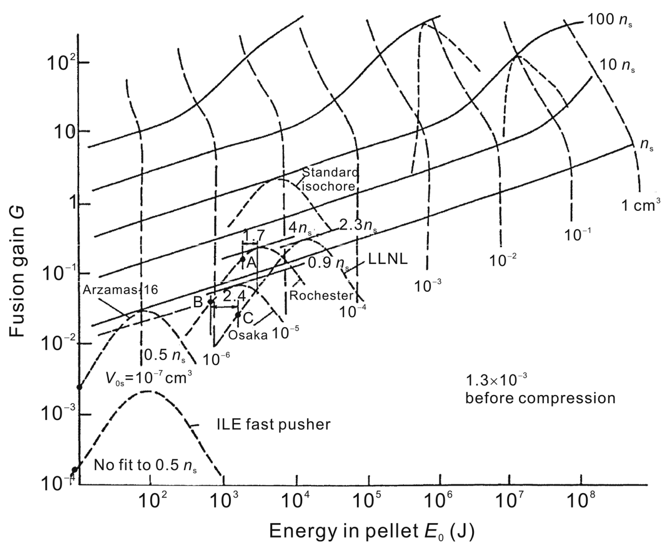

Fig. 3. Optimized core fusion gains G (full lines) for the three-dimensional self-similar hydrodynamics of volume compression for simple burn ($G < 8$) (sometimes called quenching: [40,41] and volume ignition (for $G > 8$). The measurements from Rochester [42] (point A), Osaka [43]) (point B), Livermore [44] (point C) and Arzamas-16 [45] all agree with this isentropic volume burn model, while the earlier fast pusher [46] with strong entropy-producing shocks does not agree [47].

line in Fig. 3. These straight lines combine all optimum gains at the same n/n_s resulting in gains

$$G = (\text{fusion energy})/E_0. \tag{2}$$

The justification for using the self-similarity model, as done by Basov and Krokhin [5] and Dawson [6], was clarified mathematically [7,35−38]. The gain at fixed initial density n_0 depending on the input energy E_0 for a volume V_{0s} of the fuel sphere is shown in Fig. 3 [7]. The optimum gain G is given by the just explained asymptotic tangential envelop line of the parabolic curves in Fig. 3 resulting for DT fuel in

$$G = 1.47 \times 10^{-17} E_0^{1/3} n_0^{2/3}, \tag{2a}$$

where E_0 is in J and n_0 in cm^{-3}. This could be seen from the plots shown in Ref. [7] and was published in the form of Eq. (2a) [7,38,39]. It was noted in 1964 [7] that the gains for very few special cases calculated before by Basov and Krokhin [5] and Dawson [6] were in agreement with the plots [7] in the related parabolas shown in Fig. 3 − but at much lower gains than the optimized values at the envelope. The maximum gains G in Eq. (2) results only from the envelope.

On writing Eq. (2a) energy E_0 normalized to the break-even energy E_{BE} and the density of the highest compression normalized to the solid-state DT density $n_s = 6 \times 10^{22}\ \text{cm}^{-3}$ (corresponding to a density $\rho = 0.25\ \text{g}\cdot\text{cm}^{-3}$), the following was obtained before 1971

$$G = \left(\frac{E_0}{E_{BE}}\right)^{1/3} \left(\frac{n_0}{n_s}\right)^{2/3}, \tag{3}$$

where the break-even energy $E_{BE} = 6.3$ MJ if the compression and expansion are calculated and the optimum temperature

$T_0 = T_{opt} = 17$ keV, where a Maxwellian equilibrium has been chosen corresponding to the above-mentioned envelope lines. We mention further that the energy E_0 can be expressed as

$$E_0 = 3kT_0 n_0 \frac{4}{3}\pi R_0^3, \tag{4}$$

$$G = \text{const} \times n_0 R_0. \tag{5}$$

We see that this is algebraically identical with Eq. (3), where the constant in Eq. (3) has to be taken for the optimized temperature T_{opt}. It should be noted that the nR criterion (or ρR when using the DT density ρ instead of the particle density n) for inertial-confinement fusion as a substitute for the Lawson criterion for magnetic confinement fusion was first published by Kidder in 1974 [48], and at nearly the same time by Fraley et al. [36] as a result of extensive analysis and computation. As shown in Eqs. (3)−(5), this formulation is algebraically fully identical with Eq. (2a) published in Refs. [35,39].

All the mentioned computations for direct drive spherical DT fuel adiabatic hydrodynamics and fusion reactions culminating in the gain Eq. (3) [39] − algebraically identical with Kidder's [48] ρR-formula Eq. (5) expressing the macroscopic desity ρ by n_0 − are very simplified neglecting the re-absorption of the generated bremsstrahlung within the reaction volume and the reheat there by the generated alpha particles from the reaction. Taking this into account [12,13,40,49], it leads to the discovery of volume ignition at the just discussed direct drive with complete reconfirmation by John A. Wheeler's analysis [50]. This volume ignition is primarily due to the alpha reheat and can be seen in Fig. 3 in the dashed curves being deformated form the parabolas in the lower left part of the figure. The parabolas just underlined are the result for Eq. (3) if no selfheat and re-absorption by bremsstrahlung is significant. At higher E_0 and for higher gain $G > 8$, the deformation of the parabolas begins as threshold for the volume ignition:

$$G > 8. \tag{6}$$

The dashed parabola for E_0 maximum compression density $n = 100n_s$ shows a strong upwards bent like a resonance mechanism. When printing out the temperature for a laser energy of 30 MJ on time for a number of cases close to the parameters, a jump of the temperature happens mostly due to the reheat as shown in Fig. 4.

This elaboration underlines that conditions for increasing the fusion gains are well possible but have to be selected very precisely around essential parameters. This is interesting to be taken into account also for indirect drive [28,29] when the gain will be increased by alpha-reheat [51,52] and high-foot arrangement as in the highest gain cases of Fig. 1.

4. Hybrid ignition

Secs. 2 and 3 elaborated basic properties of the indirect and direct drive laser fusion for considering the new concept of a mixture of indirect drive and direct drive laser fusion following the work by He and collaborators [53]. The just indicated examples illustrate the complexity for selecting optimized parameters. The reference to these schemes is elaborated in order to understand the possible advantages of the laser fusion scheme with picoseconds laser pulses described in the following section.

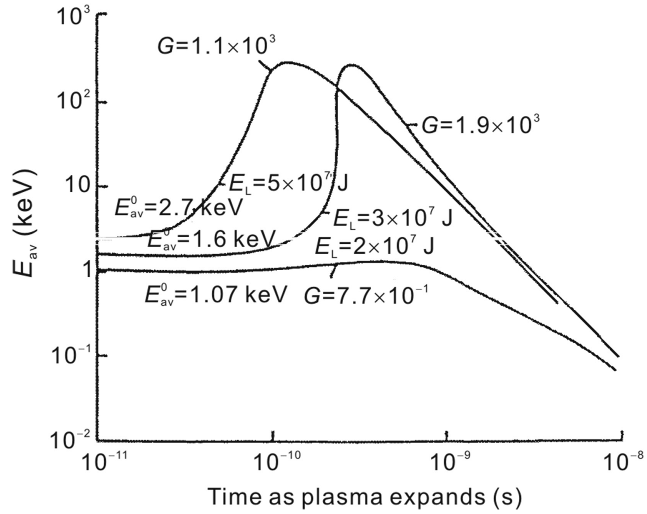

Fig. 4. Time dependence of the temperature (expressed by the internal average energy E_{av}) for a spherical DT plasma of volume 10^{-3} cm^3 at an initial compression to 5.8 × 1025 cm^3 (103 times the solid-state density) when an energy E_0 is put into the volume (equivalent to E_0) [49]. G is the resulting core gain (total generated fusion energy per $E0$). Superscript zero indicates initial values.

This result is also interesting when using variations of other properties. Examples may be that what is happening when the indirect drive is changing the surrounding capsule from an elliptic form into a spherical geometry [54]with interesting changes of the fusion reaction gains, and when in addition to the properties of the new hybrid concept the selection of the optimized parameters for volume ignition is important. The computations for the results of Fig. 3 are using only the alpha particle reheat, not including the reheat mechanism due to the generated neutron production. The results with neutrons [55] at the same values as done in a very different way of computations [56,57] show an increase of the fusion gains of about a factor of 2. From a more general view − if not considering the sensible parameters in the range of the resonance like and high peak dashed curves of Fig. 3 − in Eq. (3), a change of the fusion gain G by a factor of 2 corresponds to the necessary change of the energy input, by a factor of 8. In numbers of a fusion reactor, such a change of the driver energy is therefore an important factor.

The elaboration of the hybrid fusion ignition offers then many new aspects for laser fusion. This is not only due to the fact that indirect drive is based on the experimentally achieved proof of the inertial fusion scheme [24] for using laser energy as the driver, but to aim more refined conditions for controlled reactions in power generators where the driver energy of the radiation pulses could go down to 10 MJ or lower values. Very much has been achieved with the most advanced experiments under the leadership of the largest laser NIF ever built on earth

[28–30]. After having summarized some essential points of direct drive volume ignition (see Chapter 9 of Ref. [31] where the developments have reached powerful details [53,58] including a summarizing direction of how direct drive may give some marks for increasing the fusion gains of the very heavily developed position of indirect drive with initially expected higher gains [51].

The new hybrid-drive (HD) non-isobaric ignition scheme of inertial confinement fusion (ICF) was elaborated [53], in which a HD pressure to drive implosion dynamics increases via increasing density rather than temperature in the conventional indirect drive (ID) and direct drive (DD) approaches. In this HD (combination of ID and DD) scheme, an assembled target of a spherical hohlraum and a layered deuterium-tritium capsule inside is used. The ID lasers first drive the shock to perform a spherical symmetry implosion and produce a large-scale corona plasma. Then, the DD lasers, whose critical surface in ID corona plasma is far from the radiation ablation front, drive a supersonic electron thermal wave, which slows down to a high-pressure electron compression wave, like a snowplow, piling up the corona plasma into high density and forming a HD pressurized plateau with a large width. The HD pressure is several times of the conventional ID and DD ablation pressure and launches an enhanced precursor shock and a continuous compression wave, which give rise to the HD capsule implosion dynamics in a large implosion velocity. The hydrodynamic instabilities at imploding capsule interfaces are suppressed, and the continuous HD compression wave provides main $p\mathrm{d}V$ work large enough to hotspot, resulting in the HD nonisobaric ignition. The ignition condition and target design based on this scheme are given theoretically and by numerical simulations. It shows that the novel scheme can significantly suppress implosion asymmetry and hydrodynamic instabilities of current isobaric hotspot ignition design, and a high-gain ICF is promising [53].

The hybrid ignition demonstrates how a laser pulse with 1.37 MJ energy can produce 15 MJ fusion energy. Pressures in the range of 800 Mbar are produced and maximum implosion velocities of 400 km/s are reached. This is similar to a comparable case of direct drive with 150 km/s [30]. The layered fuel capsule is first compressed by indirect drive and then in the final stage by combining with direct drive. Attention is given to the fact that indirect drive follows an isobaric compression while the non-igniting, only burning case ($G < 8$ in Fig. 3 with the parabolas) is shown to be isochoric as shock-free self-similarity dynamics.

5. Direct drive with picosecond block-ignition for boron laser fusion

Being aware of the extensive inertial fusion (ICF) results of direct and indirect drive with spark or volume ignition, the different approach by plasma block ignition is considered. This is to some extent related to the similarities of ion driven ICF [59–62] including lasers or the FAIR (Facility for Antiproton and Ion Research) project [63,64] and developments of fast ignition [64].

For the following new aspects with boron fusion, it took dozens of years to realize the basic difference between the thermodynamic dominated laser fusion with nanosecond pulses in contrast to the entirely different non-thermal processes with the thousand times shorter picosecond laser–plasma interaction. For ns interaction of all cases described before, the laser energy has to be thermalized to produce ion pressures for the hydrodynamics and gasdynamic pressures for ablation, compression, heating and thermonuclear reactions. The problems with thermodynamics were explained by Teller and the problems for stabilizing complex systems by May [65,66] – now Lord May of Oxford – (see pages 2 and 3 of Ref. [31]). These problems can be reduced if the processes are performed within very short times such that the problematic mechanisms don't have sufficient time to develop. For laser–plasma interaction for fusion, the critical times of the interaction are changing from nanoseconds to the thousand times shorter picoseconds. Indeed, the specific properties of hydrodynamics are well included during the picosecond and shorter interaction process and in all the later processes in the plasma are following hydrodynamics and nuclear reaction processes after the picosecond initiating laser pulse interaction of the generated plasmas.

During the interaction, the dominating forces are not of thermodynamic nature but of the non-thermal electrodynamics of the laser fields with the plasma including the temporally and spatially changing dielectric conditions on densities and temperatures by the electric E and magnetic H fields form the laser of frequency ω. The force density f in the plasma is given by gas-dynamics expressed by the thermal pressure p and by the force f_{NL} by Maxwell's stress tensor as Lorentz and gauge invariant nonlinear force determined by quadratic terms of fields [67,68].

$$f = -\nabla p + f_{\mathrm{NL}} \tag{7}$$

$$\boldsymbol{f}_{\mathrm{NL}} = \nabla\cdot\left\{\boldsymbol{EE} + \boldsymbol{HH} - 0.5\left(\boldsymbol{E}^2 + \boldsymbol{H}^2\right)\mathbf{1} + [1 + (\partial/\partial t)/\omega]\left(n^2 - 1\right)\boldsymbol{EE}\right\}/(4\pi) - (\partial/\partial t)\boldsymbol{E}\times\boldsymbol{H}/(4\pi c), \tag{8}$$

where $\mathbf{1}$ is the unity tensor and n is the complex optical constant of the plasma given by the plasma frequency ω_{p}. At plane laser wave interaction with a plane plasma front, the nonlinear force reduces to showing how the force density is given by the negative gradient of the electromagnetic laser-field energy-density including the magnetic laser field from Maxwell's equations. E_{v} is the amplitude of the electric laser field in vacuum after time averaging. The second expression in Eq. (8) is the formulation of the ponderomotive force in 1845 for electrostatics of Thomson (later Lord Kelvin) that had to be later generalized to time dependence, magnetic fields with Maxwells theory, and with the dielectric properties of plasmas [13].

$$f_{\mathrm{NL}} = -(\partial/\partial x)\left(\boldsymbol{E}^2 + \boldsymbol{H}^2\right)/(8\pi) = -\left(\omega_{\mathrm{p}}/\omega\right)^2(\partial/\partial x)\left(E_{\mathrm{v}}^2/n\right)(16\pi), \tag{9}$$

Predominance against thermo-kinetic forces in Eq. (7) is possible only by laser fields of sufficiently high intensities. This is the case when the energy of electrons is larger from the quivering motion in the laser field than the energy from thermal motion in the plasma which fact is fully realized [69] and reproduced by computations (see Fig. 5). During the interaction time of 1.5 ps, the plasma reached velocities above 10^9 cm/s showing the ultrahigh acceleration $>10^{20}$ cm/s^2. The dynamic development of temperature and density has accelerated the plasma block of about 15 vacuum wavelengths thickness of the dielectric enlarged skin layer moving against the laser (positive velocity) and another block into the plasma (negative velocity) showing ultrahigh $>10^{20}$ cm/s^2 acceleration [13] (see Fig. 8.4 of Ref. [31]). The generation of the plasma blocks, one moving against the laser light and the other into the higher density target is the result of a non-thermal collisionless transfer of laser energy into plasma motion (absorption) and should not be understood as radiation pressure acceleration but as a dielectric explosion driving the plasma blocks.

The experimental proof of this ultrahigh acceleration was possible [70] in full agreement with the results of computations in 1976 by using a laser pulse of 0.3 ps duration and an intensity as in Fig. 5 [71]. These pulses were produced by Chirped Pulse Amplification CPA [72−74] with a more detailed evaluation [71]. The ultrahigh acceleration could be seen from the Doppler shift of the reflected light from the plasma block moving against the laser light. The next important result of the measurement of 1978 in Fig. 5 was that the plasma block had a thickness of about 15 vacuum wavelengths. This was skin layer with the dielectrically swelled laser wavelength in the plasma surface as an expression of the dielectric explosion between the two plasma blocks − one moving against the laser and the other moving into the interior of the plasma layer. This expressed the contrast to radiation pressure mechanisms (see pages 10 and 102 in Ref. [31]). Exactly the not varying thickness of the optical property of the skin layer was experimentally confirmed by the significant experiment [75] that the number of the accelerated ions in the blocks did not change when varying the laser intensity.

The generation of the plasma blocks and their properties was theoretically and experimentally clarified for application to the computational results [10,11], of how the fusion reaction can be initiated by irradiation on solid density fuel. Without knowing the properties of the later clarified plasma block, it was clarified that the initiation of the fusion flame is needed and the energy flux density for DT of energy can be seen from the computer output [10] (see Fig. 6). The condition for ignition is that the ion temperature >8 keV according to the included bremsstrahlung emission without re-absorption for the thin skin layer at the picoseconds initiation of the fusion flame needing a temperature >4 keV. The computations of 1971 have to be updated by later discovered phenomena, e.g. by the inhibition factor of thermal conduction in inhomogeneous plasmas [8,73] arriving at lower thresholds of E^*, referred to Eq. (10) by up to a factor of 20 (see Fig. 7).

$$E^* > 5 \times 10^8 \ \mathrm{J/cm^2} \tag{10}$$

A very surprising result was received that instead of the fusion cross for DT, those of HB11 were used. From thermally driven ICF of HB11 with nanosecond laser pulses [76] it was well known that this was more difficult against DT by very many orders of magnitudes. However, when using the non-thermal picoseconds laser pulses with nonlinear force driven block ignition, the threshold of E^* for HB11 [8,9]; were of nearly the same values. The diagrams of the kind of Fig. 6 for HB11 resulted in much higher temperatures than for DT at values of 85 keV according to a minimum temperature of 62 keV for low density compensation of reaction energy against bremsstrahlung emission.

These computations were based on one-fluid hydrodynamics as in the case of Ref. [10]. When using the basically new genuine two fluid hydrodynamics [77,78] − with showing

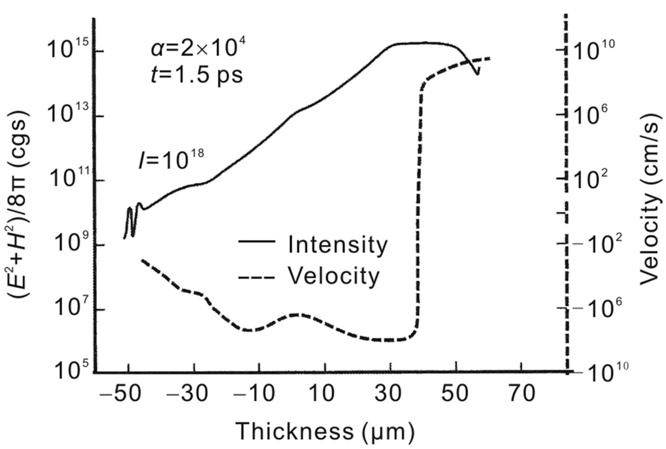

Fig. 5. 10^{18} W/cm^2 neodymium glass laser intensity in one dimensional geometry is incident from the right hand side on an initially 100 eV hot deuterium plasma slab of initially 0.1-mm -thickness whose initial density has a very low reflecting bi-Rayleigh profile, resulting in a laser energy density and a velocity distribution from plasma hydrodynamic computations at time $t = 1.5$ ps of interaction. The driving nonlinear force is negative of the energy density gradient of the laser field $(E^2+H^2)/8\pi$.

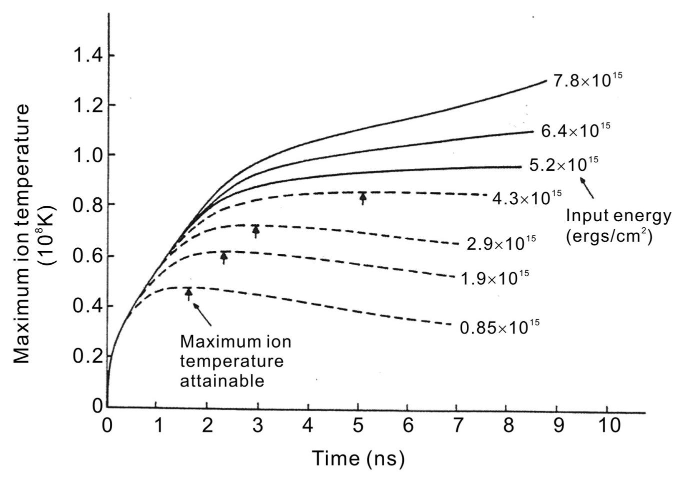

Fig. 6. Maximum ion temperature of the plasma at fusion reaction after ignition of solid density DT depending on time after the deposition of an input energy flux density E^* during 1 ps at the surface of the fuel depending on time. Decaying dashed curves show no ignition and fully drawn curve above a threshols of $E^* = 5 \times 10^8$ J/cm^2 are in the range of ignition according to Chu, 1971 [10], (see Ref. [31], Figs. 8 and 9).

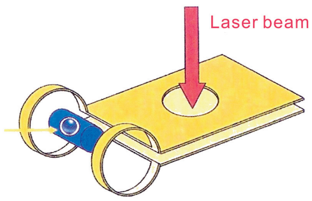

Fig. 7. Irradiating a kJ nanosecond laser pulse into the hole between the plates produces a current in the coils with 4.5 kT magnetic field being used for trapping a coaxial cylindrical plasma within the coil [20,81,82,83,84].

the internal electric fields inside of inhomogeneous plasmas (in contrast to a preceding dogma in plasma physics [31]) − the preceding results were confirmed but numerous more details were derived [79]. This referred to the generation of shocks with broadening of the shock front in generalization of the Rankine-Hugonot approximation or the few 100 ps delayed build-up of the shock with velocities much above 1000 km/s [31].

And the surprising result was even based on the pessimistic assumption, that only binary fusion reactions were used for HB11 as in the case of DT. About a further advantage of avalanche reactions specific for DT, we shall come back in the following.

A problem was that all the mentioned conditions at this stage were based on one-dimensional geometry for the laser irradiation and the target. When working with laser beams, the lateral interaction of the beam has to become under control. The alternative use of spherical geometry [83,84] needed a sufficient amount of fuel and required then more than Exawatt laser pulses for modest gains up to 500. In this situation it was most fortunate that the cylindrical trapping of the fusion reaction was possible in order to apply all the results of the infinite plane wave geometry with direct drive irradiation by a laser pulse now to the conditions of not necessarily low laser beam cross sections. The measurement of 4 kT magnetic fields in few cubicmillimeter volumes during nanoseconds [80] opened the possibility for cylindrical trapping of the fusion plasma (see Fig. 7).

The fusion reaction in the fuel cylinder can be initiated by block-ignition with end-on irradiation of picosecond laser pulses of few dozens of Petawatt power. Computations with expansion of the plasma along the radial cylindrical coordinate resulted in sufficient magnetic trapping, at least in this one dimensional model. Computations for the orbital motion may be limited by Helmholtz-Kelvin instabilities. The following results can be mentioned from the one-dimensional model along the radial dimension with the simplified assumption that the magnetic field outside the reacting volume is constant. The temporal evolution of the magnetic field due to the plasma interaction within the reaction volume was achieved to determine the reaction gains for HB11. The magnetic field in the fuel for the dynamically varying radius outside the reaction was assumed to be in vacuum.

Depending on the radius, the resulting density profiles of electrons, protons, boron ions and the resulting alpha particles were plotted in a sequence of time steps. For the end-on ignition an intensity of 10^{20} W/cm^2 was assumed for a laser wave length of 248 nm and a trapping magnetic field of 10 kT was used in most of the cases while well testing other cases with variation of the magnetic field.

The results [31] showed that for a fuel of 5 mm cylindrical radius and a laser block initiation radius of 1 mm, the plasma was completely trapped until 100 ps and the radius had grown to twice the value at 1000 ps. For the more extreme case of initiation radius of 0.1 mm, a slow radial expansion of the plasma against the magnetic field was seen from the density profile of the alpha particles of about 100 times lower than the electron density of the reacting plasma. The increase of the alphas on time demonstrated the ignition, though the computations implied pessimistically only binary fusion reactions (see Fig. 8). It should be noticed that direct drive of a fusion capsule within a high magnetic field increased the gain by a factor of 3 [85].

In conclusion, it may be clarified within the assumed conditions, that the ultrahigh magnetic fields [80] are sufficiently trapping and thermally isolating the cylindrical fusion reaction which are initiated by 30 Petawatt-ps laser pulses [15] of 100 μm radius. This is a direct drive plane geometry laser-fusion where the lateral radial energy losses of the reaction are sufficiently suppressed by the ultrahigh 10 kT magnetic fields.

6. Avalanche increase of fusion gains for a boron-laser-fusion reactor scheme

Up to this stage of the considerations, the earlier known results of direct drive block ignition by non-thermal nonlinear force produced ultrahigh acceleration, together with the ultrahigh magnetic fields for trapping are the essential ingredients for a new type of a fusion power reactor. On top the three-alpha particle HB11 reaction with equal energies to the three-alpha particles (helium ^{4}He) was measured precisely by Oliphant and Lord Rutherford in 1933 [86] after several earlier

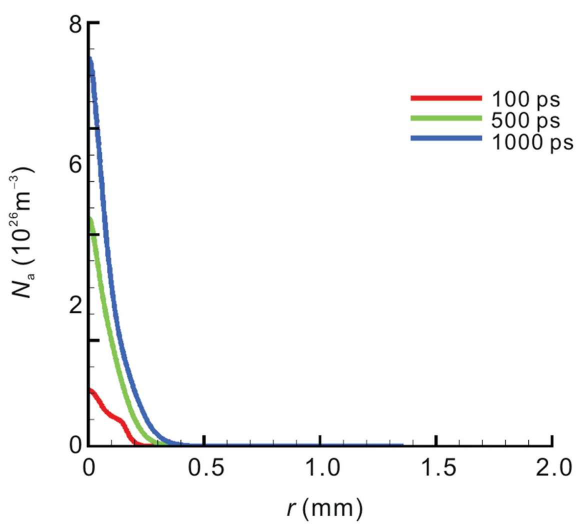

Fig. 8. Alpha particle density N_a depending on the radius r at different times (from lowest to highest curves for 100 ps, 500 ps and 1000 ps respectively) showing ignition from the increase of the curves on time [15].

suggestions of a list of nuclear reactions were observed when bombarding light elements with beams of protons of less than MeV energy. This rare case of three-alphas (or tri-alpha [87,88]) was always assumed to lead to secondary reactions by an avalanche with very high gains if the stopping lengths of alpha particles were not too short. In condensed matter, the short stopping length is well known and the question remained was how the conditions of high temperature plasmas are basically different to permit the avalanche. Estimations were presented under simplified theoretical assumptions [16].

$$^{1}\mathrm{H} + {}^{11}\mathrm{B} = 3\,{}^{4}\mathrm{He} + 8.7\,\mathrm{MeV}$$

Before going into the study of various assumptions, there were experimental results demonstrating the avalanche process. Though the HB11 fusion was highly desired for the clean environment, not a single one of the numerous proposals for using low density plasmas with magnetic confinement MCF or modifications with non-equilibrium ion beam properties could measure HB11 reactions! The very first detection of alpha particle generation was with high density plasma experiments using lasers. The first experiment by Belyaev and associates in 2005 [89] measured 1000 reactions per laser shot, just above the threshold of the sensitivity of the detection. The next measurement was by Christine Labaune and associates 2013 [17] with more than one million reactions and the measurement by Picciotto and associates in 2014 [18] resulted in one billion reactions. This number showed an energy gain of HB11 above the very high level of DT laser fusion at comparable conditions such that the summarizing comparison led to the conclusion of the avalanche reaction [19,83,90].

There are most unique advantages for the HB11 fusion compared with any other fusion reactions. The dominating number of the resulting alpha particles are of an exceptionally low energy that nuclear reactions with other nuclei apart those with protons are not occurring in these plasmas. On the other hand HB11 has a fusion reaction cross section with protons within a very broad energy range around the special value of 600 keV that is of up to 10 times higher than all other fusion reactions. The temperature within the magnetically trapped cylindrical reaction plasma of Fig. 7 for times around a nanosecond is primarily very much lower than 600 keV [18]. The energy $E_a = 2.9$ MeV of the alpha particles of the initial reactions distribute their energy by elastic collisions. As known form comparable conditions with the case of binary fusion reactions as in Fig. 8, the density of the alpha particle fluid within the reaction plasma is more than 100 times lower than in the reaction plasma whose equilibrium temperature is very far below 600 keV. This non-ideal plasma state [91,92] allows a sufficient long stopping length [93,94] such that the elastic nuclear collisions are permitting a high degree of avalanche reactions between alphas and proton within the very wide range around 600 keV. The specific evaluation of these avalanche reactions [21] then reproduces the details of the HB11 reactions with avalanche of the experiments [18,95−97]. The question of the very short stopping length of alphas in condensed matter up to solid state density has then become obsolete in view of the agreement of the results with elastic collision of nuclei in the 600 MeV range with measurements. On top it was known following the evaluations of Stepanek (see p. 203 of [31]) and experimental indications by Cayzac et al. [94], that the stopping lengths by electrons in solid density plasmas at temperatures above dozens of eV are very much larger than in condensed matter.

The avalanche process can be explained [21] on the elastic central collision [95] where an initially resting ^{11}B or proton nucleus gains energy from the energy E_α of an alpha particle. After an alpha with energy $E_\alpha = 2900$ keV has its second collision with a proton and this proton collides with a boron 11, one gets in their center-of-mass system of reference an energy E_{CM} (pB^{11}) (see Fig. 9)

$$E_{\mathrm{CM}}\left(\mathrm{pB}^{11}\right) = \left(\frac{11}{12}\right)\left(\frac{16}{25}\right)\left(\frac{9}{25}\right)E_\alpha = 612.5\ [\mathrm{keV}]. \tag{12}$$

This energy is within the maximum cross section $\sigma_{\max}$ of HB11 [98] of 1.2 b. We get the energy for HB^{11} maximum cross section σ from the alpha's collisions with protons (which then collides with B^{11}) to get the fusion as the avalanche mechanism because of the multiplication through the generation of three secondary alpha particles. In this process we get two classes of proton densities, n_{p1} that does not have any alpha collision and n_{p2} that collides with alphas and got the right energy to have a p-^{11}B collision at maximum nuclear cross section [96]. It is conceivable to assume for the Prague experiment that $n_{\mathrm{p}} = n_{\mathrm{p1}} + n_{\mathrm{p2}}$ where $n_{\mathrm{p1}} >> n_{\mathrm{p2}} = n_\alpha/3$ yielding the rate equation for the alpha particles

$$\frac{\mathrm{d}n_\alpha}{\mathrm{d}t} = 3n_{\mathrm{p1}}n_{\mathrm{B}}<\sigma v>_T + 3n_{\mathrm{p1}}n_{\mathrm{B}}<\sigma v>_{NT} + 3n_{\mathrm{p2}}n_{\mathrm{B}}\sigma_{\max}u. \tag{13a}$$

The first term on the right hand side is dependent on the ion temperature created in the laser plasma interaction and the rate $<\sigma v>_T$ is given by

$$<\sigma v>_T\left[\frac{\mathrm{cm}^3}{\mathrm{s}}\right] = 6.3820\times10^{-13}\zeta^{-5/6}\left(\frac{17.7080}{T^{1/3}}\right)^2\exp\left(-\frac{53.1240}{T^{1/3}}\zeta^{1/3}\right) + 5.41\times10^{-15}T^{-3/2}\exp\left(-\frac{148}{T}\right)\zeta$$

$$= 1 + \frac{59.3570T - 1.0404T^2 + 9.1653\times10^{-3}T^3}{10^3 + 201.65T + 2.7621T^2 + 9.8305\times10^{-4}T^3},$$

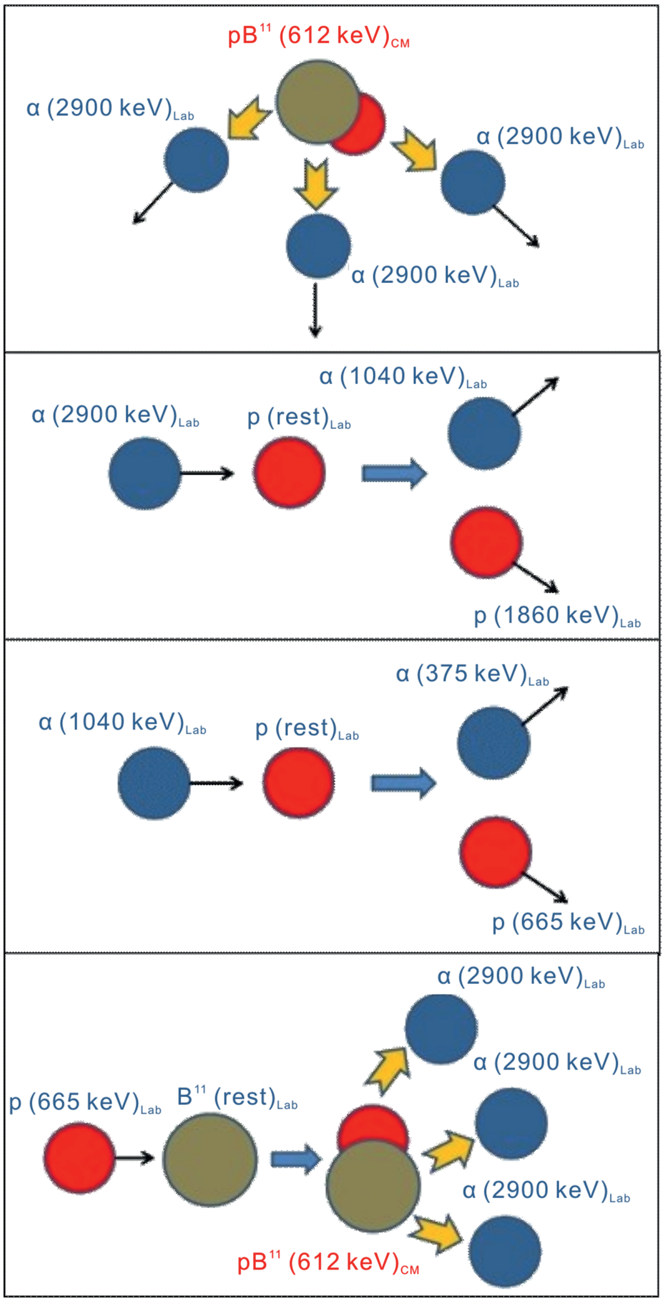

Fig. 9. A schematic overview of the avalanche process.

with ion temperature T in keV

In the Prague experiment, a total number of $N_\alpha = 4 \times 10^8$ alpha particles per laser pulse were observed from a number of protons measured experimentally as $N_H = n_p \Delta V = 10^{11}$ in a time interval of $\Delta t = 10^{-9}$ s. Calculating $N_\alpha = 3N_H n_B \langle\sigma v\rangle_T \Delta t$ according to the first term of Eq. (13a), with $n_B = 2 \times 10^{21}$ cm^{-3} at the plasma, according to hydrodynamic simulation and $\langle\sigma v\rangle_T = 6.625 \times 10^{-17}$ for $T = 100$ keV yields $N_\alpha = 4 \times 10^7$ which is an order of magnitude less than the measured N_α. Furthermore, we claim that for laser irradiance of 3×10^{16} W/cm^2 as reported in the Prague experiment an ion temperature of 100 keV is not conceivable therefore the first term in Eq. (13a) cannot explain the Prague experiment. The second term in Eq. (13a) is a non-thermal equilibrium quantity that is related to the proton spectrum measured in the Prague experiment [91]. The last term of this equation is caused by the protons that collide with the alphas and are returned back into the target by the inverted double layer (DL) simulations [78]. Therefore for processes where the non-thermal rate $\langle\sigma v\rangle_{NT}$ is dominant one has to solve to a good approximation

$$dn_\alpha/dt = 3n_{p1}n_B \langle\sigma v\rangle_{NT} + n_\alpha n_B \sigma_{max} u. \tag{13b}$$

The second term is caused by the protons that collide with the alphas while the first term in this equation is caused by protons created in the laser plasma interaction and are returned back into the target by the inverted double layer (DL) simulations [78]. Taking the data from the experiment [91], Eq. (13) can be solved numerically. In particular, the proton energy distribution as given in this experiment can be written as $dN_p/dE = N_0$ [MeV^{-1}] for $0 < E < 1$ MeV and $dN_p/dE = 0$ for $E > 1$ MeV, where n_p is the proton volume integrated density number and $N_0 = 10^{11}$ is the total number of protons under consideration. This distribution implies

$$\frac{\langle\sigma v\rangle}{\sigma_{max}u} = \frac{\int_0^\infty f(E)\sigma(E)E^{1/2}dE \Big/ \int_0^\infty f(E)dE}{(1.2\,[\text{barn}])\sqrt{0.6\text{ MeV}}} \approx 0.4. \tag{14}$$

$$f(E) = \begin{cases} N_0 = 10^{11}\,[\text{MeV}^{-1}] \text{ for } 0<E<1\text{ MeV}, \\ 0 \text{ for } 1\text{ MeV} < E. \end{cases}$$

Therefore to a good approximation we get the following solution

$$N_\alpha = \frac{\langle\sigma v\rangle_{NT}}{\sigma_{max}u} N_p\left(e^{\tau/\tau_A} - 1\right) \approx 0.4 N_0\left(\frac{\tau}{\tau_A}\right), \quad \tau_A \equiv \frac{1}{n_B \sigma_{max} u}. \tag{15}$$

N_0 is of the order of few times 10^{11} and N_α of the order of 10^9 are accordingly the volume integrated density numbers as given in the measurement in 2014 [18]; τ_A is defined as the avalanche time and the interaction time τ to create alphas. In the experiment [96], τ_A is of the order of 100 ns ($n_B = 10^{22}$ cm^{-3}, $\sigma_{max} = 1.2$ b and $u = 10^9$ cm/s) which means that alphas are created during the timescale of a nanosecond within the non-ideal plasma [93,97].

This justified in retrospect what was resulting with avalanche reactions. Using a HB11 cylinder of 1 cm length and 2 mm diameter coaxially in the coil of Fig. 7 within a magnetic field of 10 kT, the end-on irradiation of a ps laser pulse of 30 kJ focused to 200 μm diameter produces a direct drive ignition of a cylindrical reaction thermally isolated by the magnetic field. Within 1 ns, the whole fuel is reacting by the avalanche and produces more than one GJ = 277 kWh energy in alpha particles each of initially 2.9 MeV energy. The central reaction unit (see Fig. 7) is electric charged to the level of −1.4 million volts against the wall of a sphere producing alpha particles (helium nuclei) of more than a gigajoule energy, of which a small part is needed for the operation of the laser pulses. One part of the gained costs of electricity is needed for the apparatus of the central reaction and for the boron metal of the fuel being destroyed at each reaction [20,83]. If this reaction is within a reactor sphere (see Fig. 10) on a voltage of nearly −1.4 MV, the energy of the alphas − when moving against the electric field towards the reactor wall − is converted in electric power. For one reaction per second, a dc-current of 714 A has to be converted into the phases of ac-currents following the technology of HVDC (high voltage direct current) power transmission lines [99]. The process during ~1 ns within a volume of few cubic millimeters gives evidence that this can be used only for a controlled reaction for generating electricity. These considerations of direct conversion of the nuclear energy of the alpha particles into electricity is indeed the ideal mechanism. The details of the plasma state within the reactor sphere at loading the reaction units at -1.4 MV are further to be evaluated. In the worst case, the loading can be on the ground potential and the energy of the alphas is deposited in the reactor sphere just by hitting this. In this case the gained nuclear energy is then the generated heat in the reactor sphere and has to be used via heat exchangers and classical power generation.

The power reactor of Fig. 10 may then produce electricity of a value of 200−300 Million dollars per year for a profitable operation without environmental problem of nuclear radiation by using boron resources for more than thousands of years.

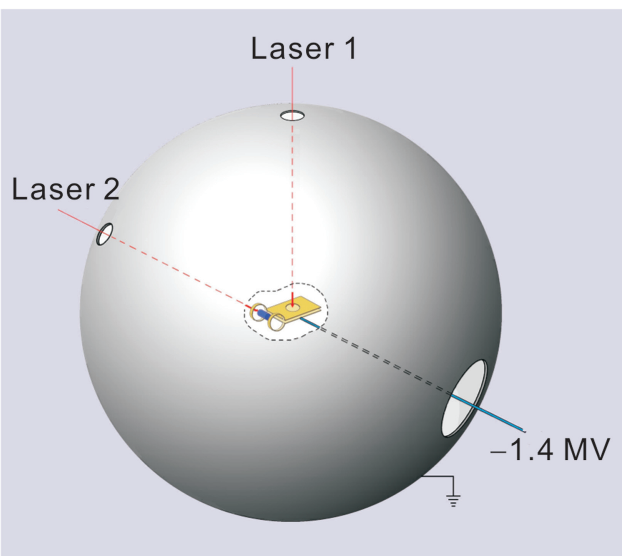

Fig. 10. The HB11 fusion without a radioactive radiation problem is based on a block ignition [71] with a 30-kJ-picosecond laser pulse 2 (see Fig. 7) where the solid hydrogen-boron fuel in the cylindrical axis of the magnetic coil is trapped by a 10 kT field sustained for about 1 ns after being generated by a laser pulse 1 of comparable duration.

7. Conclusion for developing the power reactor

To the question how close it may be to build a boron laser fusion (Bolafus) reactor (see Fig. 10), there may be a big difference to other reactor projects. The numerous laboratories for exploring laser fusion on a most sophisticated high level for the final development are presently at hand. In contrast to other projects like ITER or the Stellarator where a many years establishing of the facilities by many billion dollars investment are needed first before experimental tests for the next steps can be expected.

For the Bolafus reactor, this is basically different by the following reasons:

- the high-voltage technology in the 1.5 Megavolt current range is fully developed,
- more detailed questions about the physics of the block ignition can be continued from a lot of published results on non-thermal laser acceleration of the recent years and for more specific questions, the existing laboratories and computational capacities can immediately involve in and lead to related research and
- studies of the cylindrical fusion plasmas within the multi kT magnetic field with additional direct drive can immediately be performed in established experiments.

Even the costs for investing in additional minor equipment can be very low as well as for needed time, staff performing the studies and payment for renting of local supply.

Furthermore, the level of the needed lasers with ps pulses and dozens of Petawatts power is close to the reached value [100,101] with a repetition rate of one shot per minute [102]. Development to one shot per second with the needed high power can be expected within less than 10 years.

As in all research studies there is a probability of failure. In the case of Bolfus, the reached level is comparably advanced on many years preceding hard research such that the probability of failure is low. For the patent rights and licences all is based on very many years preceding settled knowledge but the key of combination of the non-thermal ultrahigh plasma acceleration by the nonlinear force with dielectric explosion, to be combined with known ultrahigh magnetic fields, has the legally acknowledged priority of 23 March 2014. The sufficiently high level needed for an invention is based on the fact, that just this combination only led to the breakthrough for a new power reactor of an environmentally clean, low cost and sustainable energy source.

Summarizing it was shown how the extremely powerful, ultra-short laser pulses are able to fulfil the sufficiently non-thermal plasma conditions [103] for the clean HB11 fusion at solid state density where the classical fusion energy gains are increased by **more than nine orders of magnitude** [104] with inclusion of the now experimentally and theoretically confirmed, and for the boron fusion exceptional avalanche reaction process of generating each tripling helium (alpha particles) nuclei [95]. The long known theory of ultrahigh acceleration of plasma blocks (Fig. 5 and [13,72,104]) by non-thermal direct transfer of laser energy into macroscopic motion of plasma by the nonlinear (ponderomotive) force [13,31,35,68,105] was experimentally confirmed [71] by the extremely powerful laser pulses exactly as predicted (Fig. 5 [13]) by blue shift of reflected spectral lines [62]. Combining this with the recently measured ultrahigh kilotesla magnetic fields [81] for cylindrical trapping of solid density reacting HB11 fusion plasmas, arrives at single beam ignition (Figs. 7 and 10) of several milligram boron to produce more than 300 kWh energy per shot. The advantage of the reactor of Fig. 10 consists in the fact that only one single thin picoseconds laser beam ignites the reaction by direct drive on the cylinder end of the fuel (Fig. 7), and the spherical laser irradiation for plasma compression of the other laser fusion schemes is avoided. This is the potential option for HB11 fuel to environmentally clean, low cost and lasting energy production [15,19,20,104].

References

[1] E. Teller, Memoirs, Perseus Publishing, Cambridge MA, 2001, p. 344.

[2] K. Ikeda, Progress in the ITER physics basis, Nucl. Fusion 47 (2007) S1–S404, http://dx.doi.org/10.1088/0029-5515/47/6/E01.

[3] T. Sunn Pedersen, T. Andreeva, H.-S. Bosch, S. Bozhenkov, F. Effenberg, et al., Plans for the first plasma operation of Wendelstein 7-X, Nucl. Fusion 55 (2015) 126001.

[4] M. Keilhacker, Nucl. Fusion 41 (12B) (1999) B1.

[5] N.G. Basov, O.N. Krokhin, in: P. Grivet, N. Bloembergen (Eds.), Proceedings of 3rd International Quantum Electronics Conference Paris 1963, vol. 2, 1964, p. 1375 (Dunod,Paris. 1964).

[6] J.M. Dawson, On the production of plasma by giant pulse lasers, Phys. Fluids 7 (1964) 981.

[7] H. Hora, *Abschätzungen zur Aufheizung eines Plasmas mittels Lasern* (Estmations for heating of a plasma by lasers) 1964, Report 6/23 (Institut für Plasmaphysik, Garching): Technical translation 1193 (National Research Council of Canada, Ottawa, 1965).

[8] H. Hora, Laser fusion with nonlinear force driven plasma blocks: thresholds and dielectric effects, Laser Part. Beams 27 (2009) 207.

[9] H. Hora, G.H. Miley, M. Ghorannviss, H. Malekynia, N. Azizi, X.-T. He, Fusion energy without radioactivity: laser ignition of solid hydrogen–boron (11) fuel, Energy Environ. Sci. 4 (2010) 478, http://dx.doi.org/10.1039/B904609G.

[10] M.S. Chu, Thermonuclear reaction waves at high-densities, Phys. Fluids 15 (3) (1972) 413.

[11] J.-L. Bobin, Laser Interaction and Related Plasma Phenomena, in: H. Schwarz, H. Hora (Eds.), 1974, p. 465. Plenum, New York 1975 Vol. 3A.

[12] H. Hora, R. Castillo, R.G. Clark, E.L. Kane, V.F. Lawrence, R.D.C. Miller, et al., Calculations of inertial confinement fusion gains using a collective model for reheat, bremsstrahlung and fuel depletion for high-efficient electrodynamic laser compressions, in: Proceed. 7th IAEA Conf. Plasma Phys. and Thermonucl. Fusion, Innsbruck, 23–30 August, 1978 (IAEA, Vienna, 1979), vol. III, 1979, p. 237.

[13] H. Hora, Physics of Laser Driven Plasmas, Wiley, New York, 1981.

[14] H. Hora, Skin-depth theory explaining anomalous picosecond-terawatt laser plasma interaction II, Czechosl. J. Phys 53 (2003) 199.

[15] P. Lalousis, H. Hora, S. Moustizis, Optimized boron fusion with magnetic trapping by laser driven plasma block initiation at nonlinear forced driven ultrahigh acceleration, Laser Part. Beams 32 (2014) 409.

[16] H. Hora, P. Lalousis, S. Moustaizis, I. Földes, G.H. Miley, et al., Shock studies in nonlinear force driven laser fusion with ultrahigh plasma block acceleration, in: IAEA Proceedings Fusion Energy, San Diego Oct 2012, 2012 paper IFE/P6–03, 8 pages (IAEA Vienna 2013).

[17] C. Labaune, S. Deprierraux, S. Goyon, C. Loisel, G. Yahia, et al., Fusion reactions initiated by laser-accelerated particle beams in a laser-produced plasma, Nat. Commun. 4 (2013) 2506.

[18] A. Picciotto, D. Margarone, A. Velyhan, P. Bellini, J. Krasa, et al., Boron-proton nuclear-fusion enhancement induced in boron-doped silicon targets by low-contrast pulsed laser, Phys. Rev. X 4 (2014) 031030.

[19] H. Hora, G. Korn, L. Giuffrida, D. Margarone, A. Picciotto, et al., Fusion energy using avalanche increased boron reactions for bock-ignition by ultrahigh power picoseconds laser pulses, Laser Part. Beams 33 (2015) 607.

[20] Heinrich Hora, Paraskevas Lalousis, Lorenzo Giuffrida, Daniele Margarone, Georg Korn, et al., Petawatt laser pulses for proton-boron high gain fusion with avalanche reactions excluding problems of nuclear radiation, in: SPIE Conf. Proceedings No. 9515a, paper 9515–9518, 2015.

[21] S. Eliezer, H. Hora, G. Korn, N. Nissim, J.-M. Martinez Val, Avalanche proton-boron fusion based on elastic nuclear collisions, Phys. Plasmas 23 (050704) (2016).

[22] J.H. Nuckolls, in: H. Hora, G.H. Miley (Eds.), Edward Teller Lectures, Imperial College Press, London and World Scientific Publishing Singapore, 2016, p. 85.

[23] T.H. Maiman, Stimulated optical radiation in Ruby, Nature 187 (1960) 493.

[24] Broad, W.J. 1988 New York Times 137 No. 47451, March 21.

[25] E. Cardlodge, Phys. World 29 (No. 10) (2016) 36.

[26] C. Danson, D. Hilliers, N. Hopps, D. Neely, Petawatt class lasers worldwide, High Power Laser Sci. Appl. 3 (2015) e3.

[27] S.W. Haan, T.R. Dittrich, M.M. Marinak, D.E. Hinkel, in: H. Hora, G.H. Miley (Eds.), Edward Teller Lectures, Imperial College Press, London and World Scientific Publishing Singapore, 2016, p. 262.

[28] O.A. Hurricane, D.A. Callahan, D.T. Casey, P.M. Celliers, C. Cerjan, et al., Fuel gain exceeding unity in an inertially confined fusion implosion, Nature 506 (2014) 343.

[29] D.E. Hinkel, et al., High foot implosions in larger hohlraums filled with an intermediate gas fill density, IFSA Conference, Seattle, 2016, p. 163. Sept 2015 Abstracts.

[30] J.-P. Leidinger, D.A. Callahan, L.F. Berzak-Hopkins, J.E. Ralph, P. Amendt, et al., NIF Rugby High Foot Campaign from the design side, J. Phys. Conf. Ser. 717 (2016) 012035.

[31] H. Hora, Laser Plasma Physics – Forces and the Nonlinearity Principle, second ed., SPIE Press, Bellingam WA, 2016.

[32] Nuckolls, J.H. 2009 (Discussion at ECLIM San Francisco, Sept.).

[33] J.D. Lindl, in: H. Hora, G.H. Miley (Eds.), Edward Teller Lectures, Imperial College Press London, 2016, p. 121.

[34] E. Storm, J. Lindl, E.M. Campbell, T.P. Bernat, L.W. Coleman, J.L. Emmett, et al., LLNL Livermore Report 47312, 1988.

[35] H. Hora, Plasmas at High Temperature and Density, Springer, Heidelberg, 1991.

[36] G.S. Fraley, F.J. Linnebur, R.J. Mason, R.L. Morse, Thermonuclear burn characteristics of compressed deuterium-tritium microspheres, Phys. Fluids 17 (1974) 474.

[37] H. Hora, in: H. Schwarz, H. Hora (Eds.), Laser Interaction and Related Plasma Phenomena, vol. 1, 1971, p. 427. Plenum, New York.

[38] H. Hora, D. Pfirsch, Laser energies necessary for inertially confined nuclear fusion plasmas, Sixth Int. Quantum Elect. Conf. Kyoto, Conf. Digest (September 1970) 10–11.

[39] H. Hora, D. Pfirsch, in: H. Schwarz, H. Hora (Eds.), Laser Interaction and Related Plasma Phenomena, vol. 2, 1972, p. 515. Plenum, New York.

[40] S. Atzeni, Thermonuclear burn performance of volume-ignited and centrally ignited bare deuterium-tritium microspheres, Jap. J. Appl. Phys. 34 (1986) 1995.

[41] S. Nakai, H. Takabe, Principles of inertial confinement fusion – physics of implosion and the concept of inertial fusion energy, Rep. Progr. Phys. 59 (1996) 1071.

[42] J.M. Soures, R.L. McCrory, C.P. Vernon, A. Babushkin, R.E. Bahr, et al., Phys. Fluids 31 (1996) 2884.

[43] H. Takabe, M. Yamanaka, K. Mima, C. Yamanaka, H. Azechi, et al., Scalings of implosion experiments for high neutron yield, Phys. Fluids 31 (1988) 2884.

[44] E. Storm, in: Press Conference, vol. 16, LLNL, Livermore, 1986. January 1986.
[45] G.G. Kochemasov, in: Arzamas-16 Conference, August 1996, 1996.
[46] Y. Kitagawa, Selection of Results from Gekko II (Personal Communication), 1984.
[47] Y. Kitagawa, T. Matsumoto, T. Minamihata, K. Sawai, K. Matsuo, et al., Beat-wave excitation of plasma-wave and observation of accelerated electrons, Phys. Rev. Lett. 68 (1992) 48.
[48] R.E. Kidder, Laser compression ff matter – optical power and energy-requirements, Nucl. Fusion 14 (1974) 797.
[49] S. Atzeni, Thermonuclear burn performance of volume-ignited and centrally ignited bare deuterium-tritium microspheres, Jap. J. Appl. Phys 34 (1986) 1995.
[50] H. Hora, P.S. Ray, Increased nuclear fusion yields of inertially confined DT plasma due to reheat, Z. Naturf. A 33 (1978) 890.
[51] R.C. Kirkpatrick, J.A. Wheeler, The physics of Dt ignition in small fusion-targets, Nucl. Fusion 21 (1981) 389.
[52] H. Hora, Extraordinary strong jump of increasing laser fusion gains experienced at volume ignition for combination with NIF experiments, Laser Part. Beams 31 (2013) 229.
[53] R. Betti, A.R. Christopherson, B.K. Spears, R. Nora, A. Bose, et al., Alpha heating and burning plasmas in inertial confinement fusion, Phys. Rev. Lett. 114 (2015) 255003.
[54] X.T. He, J.W. Li, Z.F. Fan, L.F. Wang, J. Liu, et al., A hybrid-drive nonisobaric-ignition scheme for inertial confinement fusion, Phys. Plasmas 23 (2016) 082706.
[55] Lan Ke, Progress in Octahedral Spherical Hohlraum Studies High Power Laser Science and Engineering Conference Suzhou March 2016, 2016. Inv. paper A-24.
[56] X.T. He, Y.S. Li, Laser interaction and related plasma phenomena, in: G.H. Miley (Ed.), AIP Conference Proceedings, No. 318, 1994, p. 334.
[57] J.M. Martinez-Val, S. Eliezer, M. Piera, Volume ignition targets for heavy-ion inertial fusion, Laser Part. Beams 12 (1994) 681.
[58] S.P. Regan, V.N. Goncharov, I.V. Igumenshchev, T.C. Sangster, R. Betti, et al., Demonstration of fuel hot-spot pressure in excess of 50 Gbar for direct-drive, layered deuterium-tritium implosions on OMEGA, Phys. Rev. Lett. 117 (2016) 025001.
[59] H. Hora, H. Azechi, Y. Kitagawa, K. Mima, M. Murakami, et al., Measured laser fusion gains reproduced by self-similar volume compression and volume ignition for NIF conditions, J. Plasma Phys. 60 (1998) 743.
[60] C. Rubbia, Heavy-ion accelerators for inertial confinement fusion, Laser Part. Beams 11 (1993) 395.
[61] M. Roth, E. Brambrink, P. Audebert, A. Blazevic, R. Clarke, et al., Laser accelerated ions and electron transport in ultra-intense laser matter interaction, Laser Part. Beams 23 (2005) 95.
[62] Yanxia Xu, Jiaxiang Wang, Xin Qi, Meng Li, Yifan Xing, Lei Yang, Wenjun Zhu, Plasma block acceleration via double targets driven by an ultraintense circularly polarized laser pulse, Phys. Plasmas 24 (2017) 033108.
[63] B.Y. Sharkov, D.H.H. Hoffmann, A.A. Golubev, Yongtao Zhao, High energy density physics with intense ion beams, Matter Radiat. Extrem. 1 (2016) 28.
[64] D.H.H. Hoffmann, in: 3rd International Conference on High Energy Density Physics, SuZhou 23–26 Sept. 2016, 2016.
[65] M. Tabak, J. Hammer, M.N. Glinsky, W.L. Kruer, S.C. Wilks, et al., Ignition and high-gain with ultrapowerful lasers, Phys. Plasmas 1 (1994) 1626.
[66] R.M. May, Will a large complex system be stable, Nature 238 (1972) 413.
[67] R.M. May, Lord May of Oxford Science and Policy Making, J. Proc. R. Soc. N. South Wales 144 (2011) 50.
[68] H. Hora, Nonlinear confining and deconfining forces associated with interaction of laser radiation with plasma, Phys. Fluids 12 (1969) 182.
[69] H. Hora, The transient electrodynamic forces at laser plasma interaction, Phys. Fluids 28 (1985) 3706.
[70] H. Hora, Distinguishing between thermalizing and electrodynamic coupling for laser-compressed thermonuclear reactions, Aust. J. Phys. 29 (1976) 375.
[71] R. Sauerbrey, Acceleration in femtosecond laser-produced plasmas, Phys. Plasmas 3 (1996) 4712.
[72] H. Hora, J. Badziak, M.N. Read, Y.-T. Li, T.-J. Liang, et al., Fast ignition by laser driven particle beams of very high intensity, Phys. Plasmas 14 (2007) 072701.
[73] D. Strickland, G. Mourou, Compression of amplified chirped optical pulses, Opt. Commun. 56 (1985) 219.
[74] G. Mourou, C.P.J. Barty, M.D. Perry, Ultrahigh-intensity lasers: physics of the extreme on a tabletop, Phys. Today 51 (1) (1998), 22.
[75] J. Badziak, A.A. Kozlov, J. Makowski, P. Parys, L. Ryc, et al., Investigations of ion streams emitted from plasma produced with a high-power picosecond laser, Laser Part. Beams 17 (1999) 323.
[76] H. Hora, B. Malekynia, M. Ghoranneviss, G.H. Miley, X. He, Twenty times lower ignition threshold for laser driven fusion using collective effects and the inhibition factor, Appl. Phys. Lett. 93 (2008) 011101.
[77] M. Kouhi, M. Ghoranneviss, B. Malekynia, H. Hora, G.H. Miley, et al., Resonance effect for strong increase of fusion gains at thermal compression for volume ignition of Hydrogen Boron-11, Laser Part. Beams 29 (2011) 125.
[78] P. Lalousis, H. Hora, First direct electron and ion fluid computation of high electrostatic fields in dense inhomogeneous plasmas with subsequent nonlinear laser interaction, Laser Part. Beams 1 (1983) 283.
[79] H. Hora, P. Lalousis, S. Eliezer, Analysis of the inverted double-layers produced by nonlinear forces in a laser-produced plasma, Phys. Rev. Lett. 53 (1984) 1650.
[80] P. Lalousis, H. Hora, S. Eliezer, J.-M. Martinez-Val, S. Moustaizis, G.H. Miley, G. Mourou, Shock mechanisms by ultrahigh laser accelerated plasma blocks in solid density targets for fusion, Phys. Lett. A377 (2013) 885.
[81] S. Fujioka, Z. Zhang, K. Ishihara, K. Shigemori, Y. Hironaka, et al., Kilotesla magnetic field due to a capacitor-coil target driven by high power laser, Sci. Rep. 3 (2013) 1170, http://dx.doi.org/10.1038/srep01170.
[82] H. Daido, F. Miki, K. Mima, M. Fujita, K. Sawai, et al., Generation of a strong magnetic-field by an intense CO_2-laser pulse, Phys. Rev. Lett. 56 (1986) 846.
[83] J.J. Santos, M. Bailly-Grandvoux, L. Giuffrida, et al., Phys. Plasmas see Ar. Xiv 1503 (2015) 00247v1.
[84] L. Giuffrida, D. Margarone, Scaling of proton-boron fusion rate using high power lasers and advance targets, Proc. SPIE 10241-13
[85] H. Hora, P. Lalousis, S. Moustaizis, Fiber ICAN laser with exawatt-picosecond pulses for fusion without nuclear radiation problems, Laser Part. Beams 32 (2014) 63.
[86] H. Hora, G.H. Miley, P. Lalousis, S. Mustaizis, K. Clayton, D. Jonas, Efficient generation of fusion flames using PW-PS laser pulses for ultrahigh acceleration of plasma blocks by nonlinear (Ponderomotive) forces, IEEE Trans. Plasma Sci. 42 (2014) 640.
[87] M. Hohenberger, P.Y. Chang, G. Fiksel, J.P. Knauer, R. Betti, et al., Inertial confinement fusion implosions with imposed magnetic field compression using the OMEGA Laser, Phys. Plasmas 19 (2012) 056306.
[88] M.L.E. Oliphant, Lord Rutherford, Experiments on the transmutations of elements by protons, Proc. R. Soc. Lond. A 141 (1933) 259.
[89] N. Rostoker, M.W. Binderbauer, H.J. Honkhorst, Colliding beam fusion reactor, Science 278 (1997) 1419.
[90] E.J. Lerner, S.K. Murali, D. Shannon, A.M. Blake, F. Van Roessel, Fusion reactions from >150 keV ions in a dense plasma focus plasmoid, Phys. Plasmas 19 (2012) 032704.
[91] V.S. Belyaev, A.P. Matafonov, V.I. Vinogradov, V.P. Krainov, V.S. Lisitsa, et al., Observation of neutronless fusion reactions in picosecond laser plasmas, Phys. Rev. E 72 (2005) 026406.
[92] H. Hora, G.J. Kirchhoff, PCT/EP2014/003281 Patent, Published as World Patent WO 2-15/144190 A1, Priority 23 March 2014, 2015.
[93] V.E. Fortov, I.T. Iakubov, The Physics of Non-ideal Plasmas, World Scientific Publ, Singapore, 2002.
[94] W. Cayzac, V. Bagnoud, M.M. Basko, S. Bedacht, A. Balzevic, et al., in: 33rd ECLIM 2014 Conf. Paris, Abstracts P. 32; Stepanek, J. 1991 Laser Interaction and Related Plasma Phenomena vol. 5, Plenum Press, New York, 2014, p. 341.

[95] S. Eliezer, H. Hora, G. Korn, N. Nissim, J.-M. Martinez Val, Response to “Comment on ‘Avalanche proton-boron fusion based on elastic nuclear collisions’”, Phys. Plasmas 23 (2016) 094703.
[96] D. Margarone, A. Picciotto, A. Velyhan, J. Krasa, M. Kucharik, et al., Advanced scheme for high-yield laser driven nuclear reactions, Plasma Phys. Contr. Fusion 57 (2015) 014030.
[97] D.H.H. Hoffmann, S. Eliezer, H. Hora, N. Nissim, V.E. Fortov, et al., in: Non-idealplasma for Avalanche Boron Fusion ECLIM Conference Moscow, Sept. 2016, 2016.
[98] W.M. Nevins, R. Swain, The thermonuclear fusion rate coefficient for p-B-11 reactions, Nucl. Fusion 40 (2000) 865.
[99] K.W. Kanngiesser, D.H. Huang, H. Lips, Hochspannungs-Gleichstromübertragungs-Systeme und ihre Planung. EV HA 7, Siemens Monogr. München (1994).
[100] C.P.J. Barty, The Nexawatt: strategies for Exawatt peak power laser based on NIF and NIF-like beam lines, in: IFSA Seattle Conf. 2015, Book of Abstracts, 2015, p. 459.
[101] Li, Ru Xin, X. Liang, Z. Gan, H. Lu, L. Yu, D. Yin, Y. Leng, X. Lu, C. Wang, Z. Xu, Progress toward a 10 PW ultra-intense laser facility: demonstration of 5 PW high gain large aperture Ti:sapphire amplifier, in: 4th Advanced Lasers and Photon Sources (ALPS'15), Yokohama, Japan, 22−24 April, 2015.
[102] T. Ditmire, Progress toward rep-related multi-petawatt lasers, Proc. SPIE (2017), 10241-25.
[103] H. Hora, Nonlinear effects and nonthermal plasmas, Nucl. Instr. Methods A271 (1988) 117.
[104] H. Hora, S. Eliezer, G.J. Kirchhoff, G. Korn, P. Lalousis, G.H. Miley, S. Moustaizis, Extreme laser pulses for possible development of boron fusion power reactors for clean and lasting energy arXiv: 1704.07224 (2017).
[105] H. Hora, Hansheng Peng, Weiyan Zhang, F. Osman, New Skin Depth Interaction by ps-TW Laser Pulses and Consequences for Fusion Energy, Dianyuan Fan, Keith A. Truesdell, Koji Yasui (Eds.), Proc. SPIE 4914 (2002) 37.